Pergamon

Cement and Concrete Research, Vol. 27, No. 3, pp. 415–426, 1997

0008-8846/97 $17.00 + .00

PII S0008-8846(97)00033-1

THERMOPHYSICAL PROPERTIES OF CONCRETE FOR NUCLEAR-SAFETY RELATED STRUCTURES

F. Vodák, R. Černý, J. Drchalová, Š. Hošková, O. Kapičková, O. Michalko, P. Semerák, J. Toman
Department of Physics, Faculty of Civil Engineering, Czech Technical University
Thákurova 7, 16629 Prague 6, Czech Republic

(Refereed)
(Received May 31, 1996; in final form January 22, 1997)

ABSTRACT

The exact knowledge of thermophysical properties of high-performance concrete for nuclear-safety related structures in wide temperature and moisture ranges is for realistic modeling of possible accidents in nuclear power plants of particular importance. In this paper, thermal conductivity, thermal diffusivity and linear thermal expansion coefficient of concrete from the French nuclear power plant Penly are determined in the temperature range from 20°C to 200°C, specific heat for -30°C to 1000°C, moisture diffusivity from 0 to 75% of maximum water saturation at room temperature, and water vapor diffusivity at room temperature. Comparison of measured results with the measurements of other authors for concretes with similar composition shows a reasonable agreement for most parameters. *©1997 Elsevier Science Ltd*

Introduction

The principal applications of concrete in nuclear safety related structures (NSRS) include its use in containment buildings, containment base mats and biological shield walls (see [1,2] for details).

Containment building represents a unique application of concrete within nuclear power plants because it encloses the entire reactor and the reactor coolant systems, and serves as the final barrier to the release of radioactive fission products to the environment under the postulated conditions of a design basis accident. The containment is designed to withstand loadings associated with a loss of coolant accident resulting from a double sided rupture of the largest pipe in the reactor coolant system. The containment is also designed to retain its integrity under low probability ($< 10^{-4}$) environmental loadings such as those generated by earthquakes, tornados and other site specific environmental events such as floods, seiche and tsunami.

The function of the containment base material (mat) is to support the reactor's internal structures and the containment building. The base mats are fabricated from reinforced concrete and generally have a thickness of 3 m or greater and a diameter of 40 m or greater.

Biological shield walls are fabricated from either standard weight reinforced concrete or heavyweight concretes. Thickness of the shield walls typically ranges from 3 m to 4 m and the walls can support either part or all the weight of the reactor vessel.

As follows from the character of nuclear-safety related structures, the requirements on their material quality are significantly higher compared to the most other concrete structures. Therefore, high-performance concrete has to be used, and both its mechanical and thermophysical properties have to be determined in wide temperature and moisture ranges in order to anticipate the behavior of NSRSs under nonstandard conditions which may occur during their lifetime.

In this paper, we have investigated the main thermal and hygric properties of high-performance concrete from the French nuclear power plant Penly (compressive strength 72 MPa - see [3]). The thermal properties were measured for temperatures from 20°C to 200°C which covers the necessary temperature range for concrete containment building in most possible accidents in a nuclear power plant [4], the measurements of hygric properties were done at room temperature in a wide range of moisture content.

Material Composition

The Penly concrete (samples were obtained from M. Dugat, Bouygues Company, France) has the volume mass of 2290 kgm^{-3}, and consists of the following components: Cement CPA HP Le Havre (290 kgm^{-3}), sand 0/5 size fraction (831 kgm^{-3}), gravel sand 5/12.5 size fraction (287 kgm^{-3}), gravel sand 12.5/25 size fraction (752 kgm^{-3}), calcareous filler PIKETTY (105 kgm^{-3}), foamed silica (30 kgm^{-3}), water (131 kgm^{-3}), retarder CHRYTARD 1.7, superplasticizer Rèsine GT 10.62.

Moisture Diffusivity

The moisture diffusivity of many materials depends dramatically on the moisture content (sometimes within the range of several orders of magnitude) which makes its determination relatively complicated.

The methods most commonly used for determining the moisture diffusivity, e.g., the steady-state method [5], and the non-steady-state methods by Matano [6], Drchalová [7], and Häupl and Stopp [8], have a common feature; they work with one - dimensional moisture transport, and calculate the moisture diffusivity from the spatial moisture distribution at one or several time intervals. Therefore, the methods require rod samples where the moisture sensors are positioned along the longitudinal axis; they completely fail when only plate samples are available. Also, the application of these techniques for materials with very low moisture diffusivity (such as concrete or various rocks) usually leads to the increasing errors as the moistening process is too slow and the spatial moisture distribution is difficult to determine with a sufficient accuracy (e.g., [7], [9], [10]).

Therefore, we have chosen a method which is suitable particularly for plate materials and requires only measuring of the time history of the water content in the sample (see [11], for details). The method is based on the assumption that the moisture diffusivity coefficient κ can be considered as piecewise constant with respect to the moisture content, and appears in the phenomenological relation

$$j = -\kappa \operatorname{grad} \rho_m = \rho_d \kappa \operatorname{grad} u, \tag{1}$$

where j is the moisture flux, ρ_m the mass of liquid moisture per unit volume (moisture density, in the sense of the classical linear theory of mixtures), ρ_d the volume mass of the dried specimen (i.e., of the porous skeleton), u the moisture content, $u = \rho_m/\rho_d$. The measurements were performed on plate-type samples, i.e., the moisture transport in the direction of the thickness of the plate can be considered as one-dimensional.

Under the assumptions given above, we can write the transport equation for a certain (not very wide) range of moisture in the form

$$\frac{\partial \rho_m}{\partial t} = \kappa \frac{\partial^2 \rho_m}{\partial x^2}, \quad x \in [0, l], \tag{2}$$

where l is the thickness of the plate sample.
The initial and boundary conditions can be defined as

$$\rho_m(x, 0) = \rho_2 \tag{3}$$

$$\rho_m(0, t) = \rho_1 \tag{4}$$

$$\rho_m(l, t) = \rho_2, \tag{5}$$

where ρ_2 is the initial moisture density in the specimen, ρ_1 is the maximum moisture density which can be achieved in the material (the bottom surface of the plate is in the direct contact with water during the moistening process).

The diffusion problem (2)-(5) can be solved analytically with the result:

$$\rho_m(x, t) = \rho_1 + (\rho_2 - \rho_1)\frac{x}{l} + \frac{2}{\pi}\sum_{n=1}^{\infty} \frac{\rho_2 - \rho_1}{n} \sin\left(\frac{n\pi x}{l}\right) \exp\left(-\frac{\kappa n^2 \pi^2 t}{l^2}\right). \tag{6}$$

The total mass of water which entered the sample during the time interval $[0, \tau]$ can be expressed by the relation

$$m_m(\tau) = S \cdot \int_0^l (\rho_m(x, \tau) - \rho_2)\, \mathrm{d}x, \tag{7}$$

where S is the area of the plate surface which is in the direct contact with water.

After substituting (6) into (7) we get the final transcendent equation for κ

$$m_m(\tau) - S(\rho_1 - \rho_2)\frac{l}{2} + \frac{2lS}{\pi^2}(\rho_1 - \rho_2)\sum_{n=1}^{\infty} \frac{1}{n^2}(1 - \cos(n\pi)) \cdot \exp\left(-\frac{\kappa n^2 \pi^2 \tau}{l^2}\right) = 0, \tag{8}$$

which can be solved by some of the iteration methods, e.g., Newton or regula falsi. The value of κ determined by the solution of (8) we identified with the characteristic average value of the moisture content in the sample in the time interval $[0, \tau]$,

$$u_c = \frac{m_m(\tau)}{2Sl\rho_d} + \frac{\rho_2}{\rho_d}. \tag{9}$$

In practical measurements we performed the experiment with a set of specimens with various values of the initial moisture density ρ_2, and determined the corresponding set of values of the moisture diffusivity $\kappa(u_c)$. In this way we obtained a pointwise given function $\kappa(u)$, i.e., the dependence of the moisture diffusivity on the moisture content.

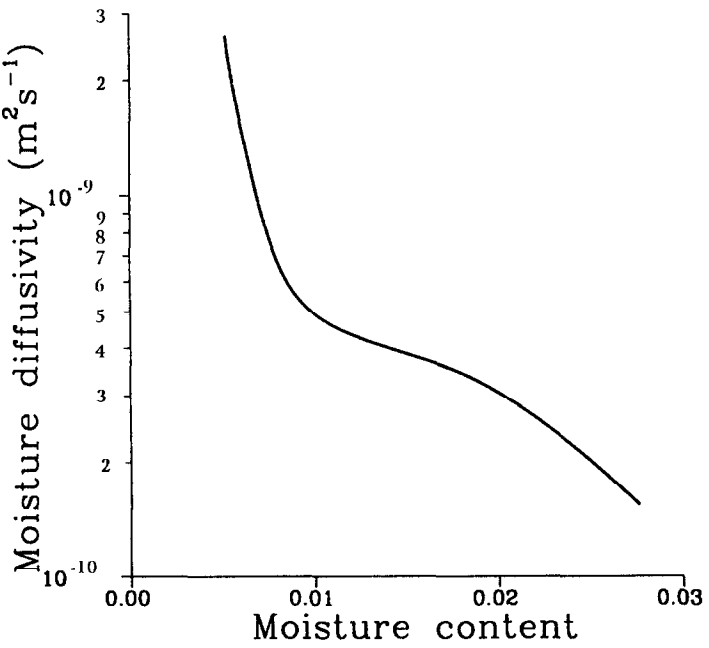

FIG. 1.
Dependence of moisture diffusivity of Penly concrete on moisture content.

The specimens for the measurements of the moisture diffusivity of the Penly concrete were prepared from the cylindrical rods which were 400 mm in length and 100 mm in diameter. The resulting plate samples were 20 mm thick and 100 mm in diameter.

The measurements were performed with the following values of the initial moisture content in the specimens: 0.0033, 0.0049, 0.0054, 0.0088, 0.0176, 0.0273. The maximum moisture content $u_{\max}$ reached by putting the specimen into water at room temperature for 7 days was 0.040.

Fig. 1 shows the dependence of moisture diffusivity of the Penly concrete on the moisture content determined by the method with piecewise constant κ described above. The function $\kappa(u)$ has apparently decreasing character, the differences between the maximum and minimum values being approximately one order of magnitude.

Water Vapor Diffusivity

Water vapor diffusivity (the diffusion coefficient of water vapor) D in a porous material is defined by the phenomenological relation

$$j_v = -D \operatorname{grad} \rho_v, \tag{10}$$

where j_v is the flux of water vapor and ρ_v is the volume mass of the water vapor in the porous material which is usually considered to be independent of the concentration of water vapor.

For measuring D we have chosen a steady-state method commonly used for other materials. The measuring apparatus consists of two airtight glass chambers separated by the sample of the measured material, which is typically plate-type. In the first chamber, a state was kept near to 100% relative humidity (achieved by placing a cup of water in the chamber), while in the second chamber the state was close to 0% relative humidity (set up by using some absorption material, such as silica gel). At given time intervals τ the measurement was interrupted, and the changes in the mass of water in the cup, Δm_w, and of the silica gel, Δm_a were checked. The experiment was terminated, when $|\Delta m_w| \sim |\Delta m_a|$, i.e., when the steady state was established within the measuring system. The experiment was carried out under isothermal conditions.

Assuming the water vapor transport to be one-dimensional, the mass of water vapor which entered the sample during the time interval $[0, \tau]$, Δm_w, can be expressed as

$$\Delta m_w = S \int_0^\tau -D \left(\frac{\partial \rho_v}{\partial x} \right)_{x=0} \mathrm{d}t, \tag{11}$$

where S is the area of the surface of sample being in contact with the environment of the specified humidity ($x = 0$ in the chosen coordinate system).

The relation between the volume mass ρ_v and the partial pressure of water vapor p_v is given by the equation of state which for an ideal gas reads

$$p_v = \frac{\rho_v}{M} RT, \tag{12}$$

where R is the universal gas constant, T the temperature in degrees K, M the molar mass of water vapor. The pressure of saturated water vapor, $p_{v,s}$, can be either found in tables or expressed by the standard formula

$$p_{v,s} = T^C \cdot 10^{-\frac{A}{T}+B}, \tag{13}$$

where the pressure $p_{v,s}$ is given in Pa and constants A, B, C have the values

$$A = 2900\ K, \quad B = 24.738, \quad C = -4.65.$$

Substituting (12–13) in (11) and taking into account the experimental conditions described we get for the diffusion coefficient D at the temperature T

$$D = \frac{\Delta m_w R l}{S \tau M \cdot T^{C-1} \cdot 10^{-\frac{A}{T}+B}}, \tag{14}$$

where l is the thickness of the plate-type sample.

Another commonly used quantity for the specification of water-vapor isolating properties of building materials is the equivalent thickness l_{eq} defined as

$$l_{\mathrm{eq}} = \frac{D_a}{D} \cdot l, \tag{15}$$

where D_a is the diffusion coefficient of water vapor in the air.

As our samples are prepared in the laboratory and do not represent any real construction element, it seems reasonable to define l_{eq} here as the thickness equivalent to, for instance, 1 cm of the measured concrete, i.e.,

$$l_{\mathrm{eq}} = 0.01 \cdot \frac{D_a}{D} \quad (m). \tag{16}$$

Measurements of the water vapor diffusivity in the Penly concrete were performed at the temperature $24 \pm 1°C$ on six plate samples, 20 mm thick and 100 mm in diameter, which were cut from the cylindrical rods 400 mm in length. The experiments on each sample were repeated three times. The mean values and standard deviations of D and l_{eq} evaluated from 18 measurements are

$$D = (4.98 \pm 0.26) \cdot 10^{-7}\ m^2 s^{-1}$$

$$l_{eq} = (0.47 \pm 0.02)\ m/1\ cm \text{ concrete.}$$

Specific Heat

The application of the classical adiabatic-calorimetry methods in measuring the specific heat of building materials can lead to certain difficulties due to the following reasons:

a) The samples of building materials have to be relatively large because of their inhomogeneity.
b) Due to the low thermal conductivity of most building materials a relatively long time is needed to reach the temperature equilibrium over large dimensions, resulting in significant heat losses.

Therefore, a nonadiabatic method was used for determining the temperature-dependent specific heat (see [12], for details).

The nonadiabatic calorimeter we used had a mixing vessel with a volume of 2.5 liters. The volume of the measuring fluid (water in this case) was about 1 liter. The maximum volume of the measured samples was 1 liter. The amount of heat loss of the nonadiabatic system was determined using a calibration.

The samples for experimental measurements of specific heat in the dependence on temperature were prepared by cutting the original rods of $100 \times 100 \times 400$ mm to the dimensions of $100 \times 100 \times 47$ mm. The reason why we have chosen this treatment was a necessity to achieve a good mixing during the preparation of the samples.

The nonadiabatic method from [12] was applied for measurements at the following initial sample temperatures: $100°C$, $200°C$, $400°C$, $600°C$, $800°C$, $1000°C$, and repeated three times for each temperature. For the initial sample temperature lower than $600°C$, the material was basically unaffected by the contact with water in the calorimeter. However, during the measurements at $800°C$, small cracks were observed on the surface of the samples. The samples heated at $1000°C$ were destroyed after putting in a contact with water in the calorimeter (the samples were split into small pieces). For the measurements of specific heat at temperatures lower than $100°C$ ($-30°C$, $0°C$), the classical adiabatic method was employed.

The experimental results which are summarized in Fig. 2 show that for the containment concrete the $c(T)$ curve has an increasing character in the whole temperature range from $-30°C$ to $1000°C$. This is an expected character of the temperature dependence of specific heat known for other types of concrete.

Thermal Expansion

The thermal expansion coefficient is defined [13]

$$\alpha = \frac{\Delta l}{l_o \Delta T}, \tag{17}$$

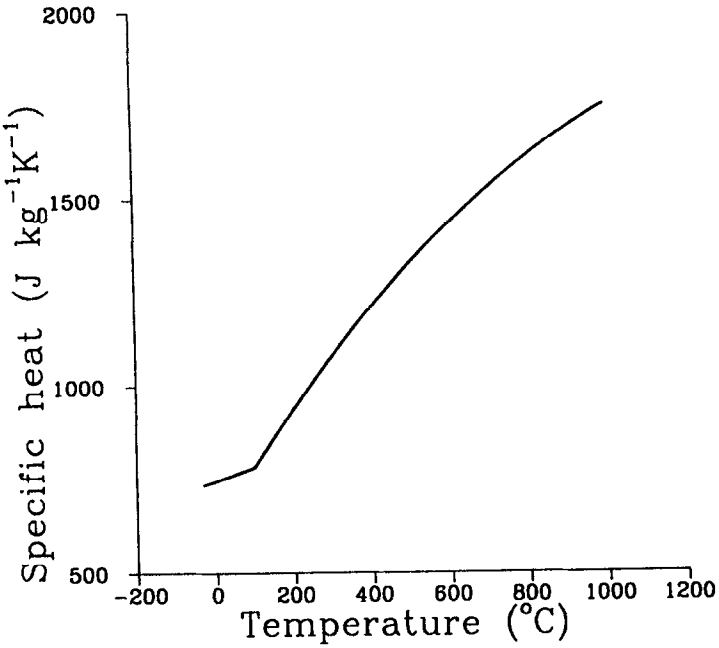

FIG. 2.
Temperature dependence of specific heat of Penly concrete.

where Δl is the change of length of the specimen caused by the temperature change ΔT, and l_o is the length of the specimen at some reference temperature, for instance 0°C. At the measurements, the sample was heated to a given temperature and when the thermal equilibrium was reached its length was determined. As the values of thermal expansion coefficient α are rather small high accuracy of the length measurement is required.

The measurements were carried out on four samples of the Penly concrete with the dimension of about 50 × 50 × 200 mm. The measurements were performed in BRABENDER KW 40 climate box at temperatures in the range [−33°C, +192°C]. Each specimen was exposed for eight hours to the predetermined temperature prior to the length measurements were carried out. The measurements of the length of the samples were performed on ZEISS contact Abbe comparator. With the specimen length 200 mm and the pressure force 0.07 N at the contact, the accuracy of the comparator is $0.1 \cdot 10^{-6}$m.

The dependence of the thermal expansion coefficient on temperature is shown in Fig. 3. No hysteresis was observed in going up and down with temperature.

Thermal Conductivity

For the measurement of thermal conductivity λ of Penly concrete, the quick thermal conductivity meter SHOTHERM QTM-D2 was used. The measurements were carried out on five samples of the Penly concrete with dimensions of 60 × 60 × 150 mm. The samples were specially prepared with respect to dimensions of the measuring probe.

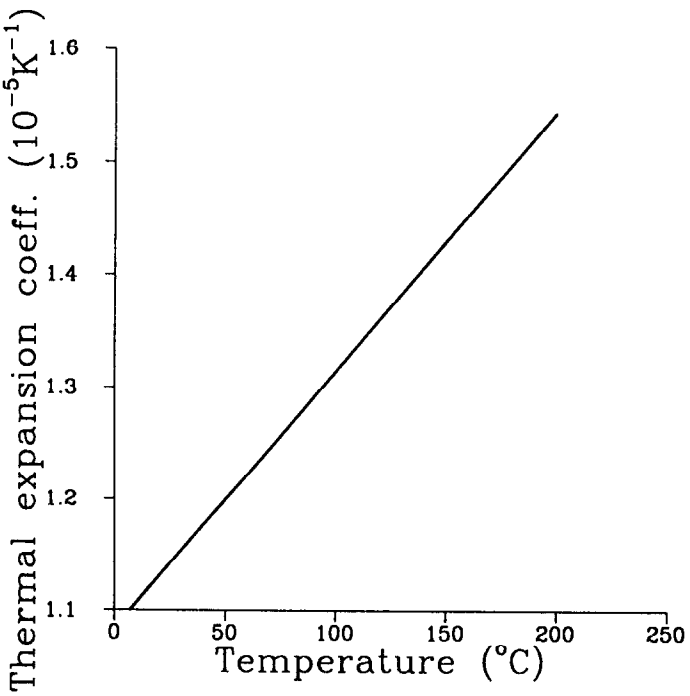

FIG. 3.
Temperature dependence of linear thermal expansion coefficient of Penly concrete.

The measurements of the thermal conductivity were performed in the BRABENDER climate box at the following initial temperatures: 30°C, 60°C, 90°C, 150°C and 200°C. Due to the nonhomogeneity of the samples, the measurements were repeated forty times at each temperature. The differences between individual values of λ and its mean value were less than 2%. Moisture content in the samples was controlled during the measurement and did not exceed the value of 0.004. The experimental results are summarized in Fig. 4. The results show that λ decreases with the increasing temperature in the whole temperature range up to 200°C. This behaviour is typical for concrete samples and agrees with our previous measurements.

The error in the thermal conductivity measurements is determined by the accuracy of the QTM meter which is 5% of the indicated value.

Thermal Diffusivity

The thermal diffusivity coefficient a is defined as

$$a = \frac{\lambda \rho}{c}, \tag{18}$$

where λ is the thermal conductivity, ρ the volume mass, and c the specific heat. In Eq. (18), temperature dependences of thermal conductivity and specific heat for the Penly concrete were taken into account. The experimental results are summarized in Fig. 5.

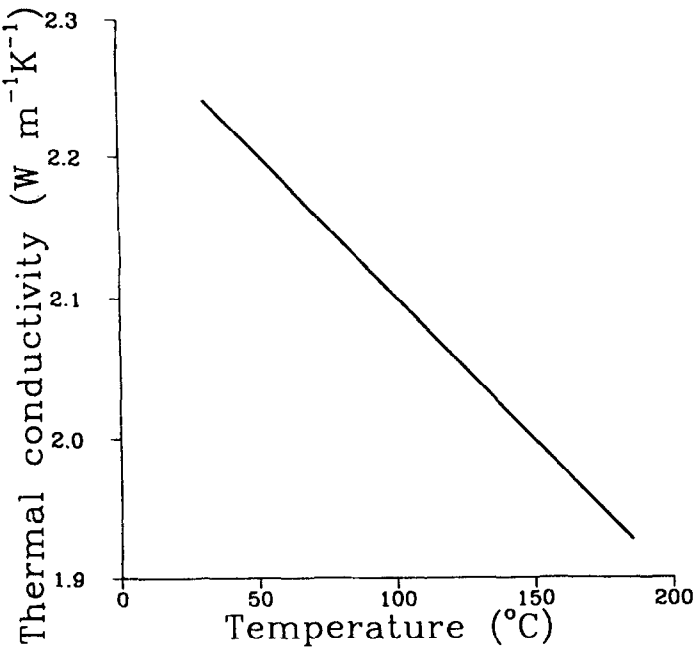

FIG. 4.
Temperature dependence of thermal conductivity of Penly concrete.

Discussion

High-temperature measurements of thermophysical properties of normal concretes (compressive strength < 40 MPa, see [14]) were frequently carried out during the last 2–3 decades (see [15] for an extensive review). However, analogous measurements for high-performance concretes are relatively sparse (e.g. [3]). Therefore, the experimental results in this paper can be compared with normal concretes mostly.

Table 1 shows a comparison of our measurements of thermal conductivity of Penly concrete with some literature data for concretes with an analogous composition (siliceous concretes). Our results are slightly lower (up to 10%) than the other ones but the same decreasing character of the $\lambda(T)$ function was observed.

TABLE 1
Comparison of Thermal Conductivity of Various Siliceous Concretes (W/mK)

Temperature (°C)	50	100	150	200
This work	2.20	2.10	2.00	1.90
Harwathy [16]	2.50	2.39	2.22	2.14
Abe et al. [17]	2.53	2.26	2.03	1.80

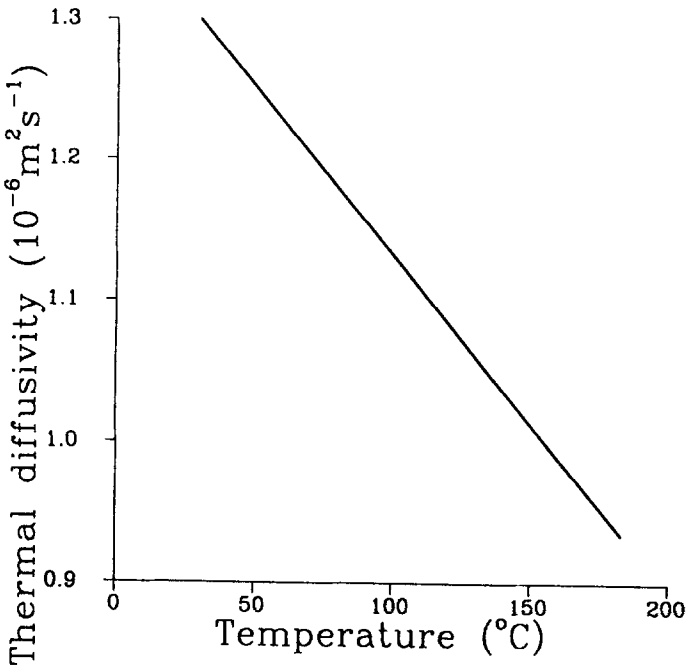

FIG. 5.
Temperature dependence of thermal diffusivity of Penly concrete.

The measured data for thermal diffusivities were for Penly concrete higher than for two chosen other concretes, as illustrated in Table 2, and the differences increased with the increasing temperature. The possible reason could be in the fact that our data were obtained by calculation from λ, ρ, c while the other ones by an analysis of temperature fields.

Specific heat of Penly concrete was a little bit lower than two other chosen concretes (Table 3), the differences ranged from 10% to 20%.

Linear thermal expansion coeffiecient ranged from $1.1 \cdot 10^{-5}$ K^{-1} to $1.6 \cdot 10^{-5}$ K^{-1} in our measurements, which is in a reasonable agreement for instance with the measurements of Zoldners et al. [21] for concrete with quartzite gravel ($1.6 \cdot 10^{-5}$ K^{-1} up to 500°C), and also with the IEA recommendations [22]($1.2 \cdot 10^{-5}$ K^{-1}).

TABLE 2

Comparison of Thermal Diffusivity of Various Siliceous Concretes ($10^{-6}m^2/s$)

Temperature (°C)	50	100	150	200
This work	1.25	1.13	1.02	0.90
Felicetti et al. [3]	1.25	0.80	0.72	0.44
Pogorzelski [18]	0.91	0.79	0.76	0.70

TABLE 3

Comparison of Specific Heat of Various Siliceous Concretes (J/kgK)

Temperature (°C)	50	100	150	200
This work	770	790	860	940
Harmathy and Allen [19]	800	950	1000	1080
Hildenbrand et al. [20]	980	1000	1020	1040

The hygric properties of Penly concrete were slightly higher than for the other concretes of similar composition. For instance, Bažant and Najjar [23] measured $\kappa = 1.16 \cdot 10^{-10}$ m^2/s while our values are higher than $1.5 \cdot 10^{-10}$ m^2/s in all range of moisture content, and the IEA recommendation [22] for water-vapor diffusion coefficient of normal concrete is $\sim 2 \cdot 10^{-7}$ m^2/s while we obtained $\sim 5 \cdot 10^{-7}$ m^2/s. This means that the porous structure of Penly concrete is probably a little bit more open than it would be expected for high-performance concrete.

Conclusions

Main thermal and hygric parameters of high-performance concrete for nuclear-safety related structures in the French nuclear power plant Penly were measured depending on temperature and moisture content. Thermal conductivity, thermal diffusivity, and linear thermal expansion coefficient were determined in the temperature range of 20°C to 200°C, specific heat for temperatures to 1000°C, moisture diffusivity for the moisture range from 0 to 75% of maximum water saturation, water vapor diffusivity for the maximum partial pressure difference between the two measuring chambres at room temperature. Most of the measured results were found to be reasonably close to the results obtained by other experimentalists for concretes with similar composition.

Acknowledgements

This work was partially supported by the International Atomic Energy Agency under contract No. 7296/R1/RB, and by the EC PECO 93 grant No. SAV 22179/VCH.

References

1. Safety Aspects of Nuclear Power Plant Ageing, IAEA-TECDOC-540, Vienna 1990.
2. D.J. Naus, C.B. Oland, Aging of Concrete Containment Structures in Nuclear Power Plants, CONF-920541-2, Fifth Workshop on Containment Integrity, Washington D.C., May 12-14, 1992.
3. R. Felicetti, P.G. Gambarova, G.P. Rosati, The Mechanical Properties of a High-Performance Siliceous Concrete Exposed to High Temperatures; "Penly" Concrete: Unaxial Compression, Research Project 1794/20-3-95, Milan University of Technology, March 1995.
4. Working material: Report #1 on the containment aging survey results (CRP on Containment Ageing, IAEA 1995).
5. I. Kaŝpar, Moisture Transport in Building Materials (in Czech). DrSc. Thesis, CTU Prague 1984.

6. C. Matano, Jap. J. Phys. 8, 109 (1933).
7. J. Drchalová, A Non-Steady-State Method for Determining the Moisture Diffusivity. PhD. Thesis, CTU Prague 1983.
8. P. Häupl, H. Stopp, Schriftenreihe der Sektion Architektur der TU Dresden 16, 93 (1980).
9. R. Černý, Second-Order Influences on the Moisture Transport in Porous Materials. Habilitation thesis, CTU Prague 1990.
10. I. Kašpar et al., Transport Phenomena in Capillary Porous Bodies (in Czech). Research Report # 145F73-75, CTU Prague 1975.
11. R. Černý, J. Drchalová, Measuring the Moisture Diffusivity of Board Materials, Proc. of the CIB W40 Meeting, Porto 1995, p.147.
12. J. Toman and R. Černý, High Temp.-High Press. 25, 643 (1993).
13. W.E. Gettys, F.J. Keller, M.J. Skove, Physics, Mc Graw Hill Book Comp. 1989.
14. P.K. Mehta, P.J.M. Monteiro, Concrete. Structure, Properties, and Materials, 2nd Edition, Prentice Hall, 1993.
15. Z.P. Bažant, M.F. Kaplan, Concrete at High Temperatures. Material Properties and Mathematical Models. Longman, 1996.
16. T.Z. Harwathy, ASTM J. of Materials 5, 47 (1970).
17. H. Abe, T. Kawahara, T. Ito, A. Haraguchi, In: Concrete for Nuclear Reactors, ACI Special Publ. No 34, Vol. 2, Paper SP34-40, p. 847. American Concrete Institute, Detroit 1972.
18. J.A. Pogorzelski, Thermal Properties of Some Building Materials. Report to RILEM Committee 44-PHT, Warsaw 1980.
19. T.Z. Harmathy, L.W. Allen, J. Amer. Concr. Inst. 70, 132 (1973).
20. G. Hildenbrand, M Peeks, A. Skokan, M. Reimann, Investigations in Germany of the Barrier Effect of Reactor Concrete Against Propagating Molten Corium in the Case of a Hypothetical Meltdown Accident of a LWR. In: ENSIANS Int. Meet. on Nuclear Power Reactor Safety, Vol. 1, Brussels, 1978, p. 16.
21. N.G. Zoldners, V.M. Malhotra, H.C. Wilson, Proc. Am. Soc. Test. Mat. 60, 1087 (1960).
22. IEA-Annex XIV., Condensation and Energy, Vol. 3, Catalogue of Material Properties. IEA, Brussels 1991.
23. Z.P. Bažant, L.J. Najjar, Nonlinear Water Diffusion in Nonsaturated Concrete. Materials and Structures, RILEM, Paris, 5, 3 (1972).